SUPPLEMENTAL MATERIALS:

Materials and Methods

Supplemental Figures S1-S13

References (42-46)

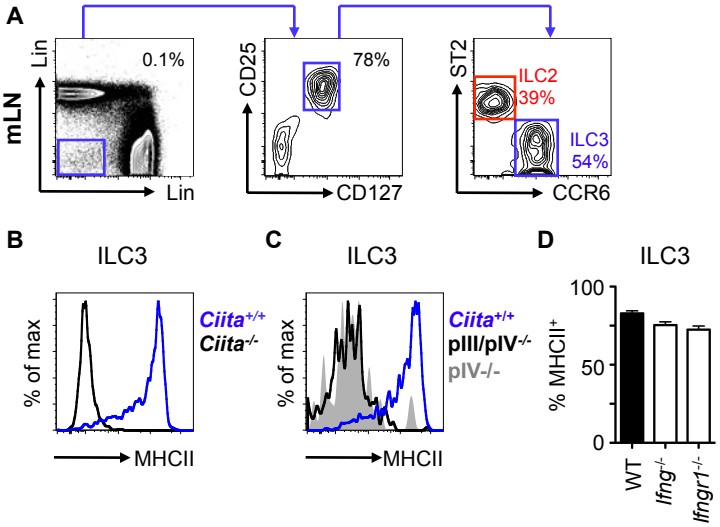
A
mLN
Lin
0.1%
Lin
CD25
78%
CD127
ST2
ILC2
39%
ILC3
54%
CCR6
B
ILC3
% of max
Ciita+/+
Ciita-/-
MHCII
C
ILC3
% of max
Ciita+/+
pIII/pIV-/-
pIV-/-
MHCII
D
ILC3
% MHCII+
100
50
0
WT
Ifng-/-
Ifngr1-/-

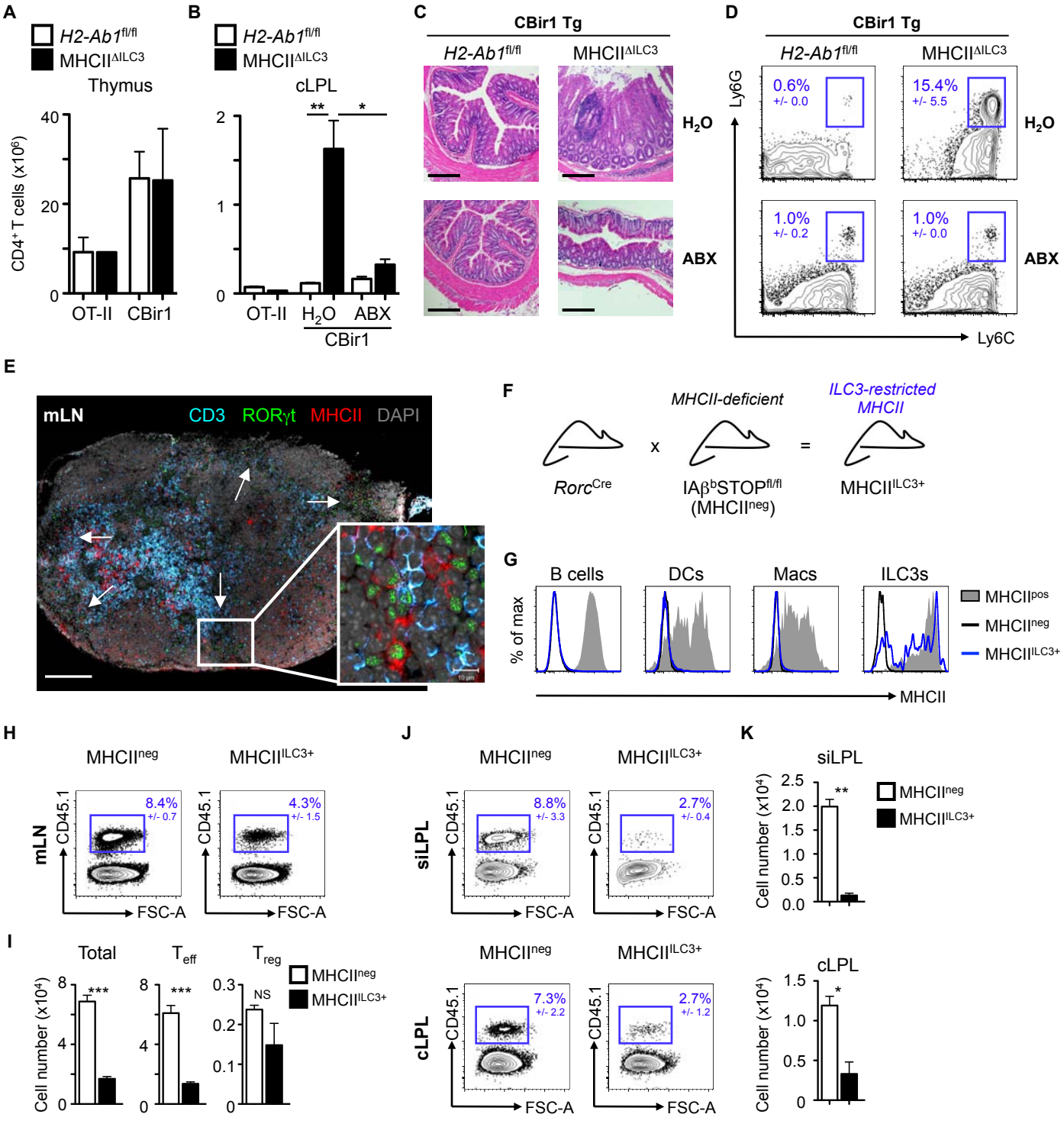
A
H2-Ab1fl/fl
MHCIIΔILC3
Thymus
CD4+ T cells (x10⁶)
40
20
0
OT-II
CBir1
B
H2-Ab1fl/fl
MHCIIΔILC3
cLPL
**
*
2
1
0
OT-II
H2O
ABX
CBir1
C
CBir1 Tg
H2-Ab1fl/fl
MHCIIΔILC3
H2O
ABX
D
CBir1 Tg
H2-Ab1fl/fl
MHCIIΔILC3
Ly6G
0.6%
+/- 0.0
15.4%
+/- 5.5
1.0%
+/- 0.2
1.0%
+/- 0.0
H2O
ABX
Ly6C
E
mLN
CD3
RORγt
MHCII
DAPI
F
MHCII-deficient
ILC3-restricted MHCII
x
=
Rorc^Cre
IAβ^bSTOP^fl/fl (MHCII^neg)
MHCII^ILC3+
G
B cells
DCs
Macs
ILC3s
% of max
MHCIIpos
MHCIIneg
MHCIILC3+
MHCII
H
MHCIIneg
MHCIILC3+
mLN
CD45.1
8.4%
+/- 0.7
4.3%
+/- 1.5
FSC-A
I
Total
Teff
Treg
MHCIIneg
MHCIILC3+
Cell number (x10⁴)
***
***
NS
J
MHCIIneg
MHCIILC3+
siLPL
8.8%
+/- 3.3
2.7%
+/- 0.4
cLPL
7.3%
+/- 2.2
2.7%
+/- 1.2
CD45.1
FSC-A
K
siLPL
**
cLPL
*
Cell number (x10⁴)
MHCIIneg
MHCIILC3+

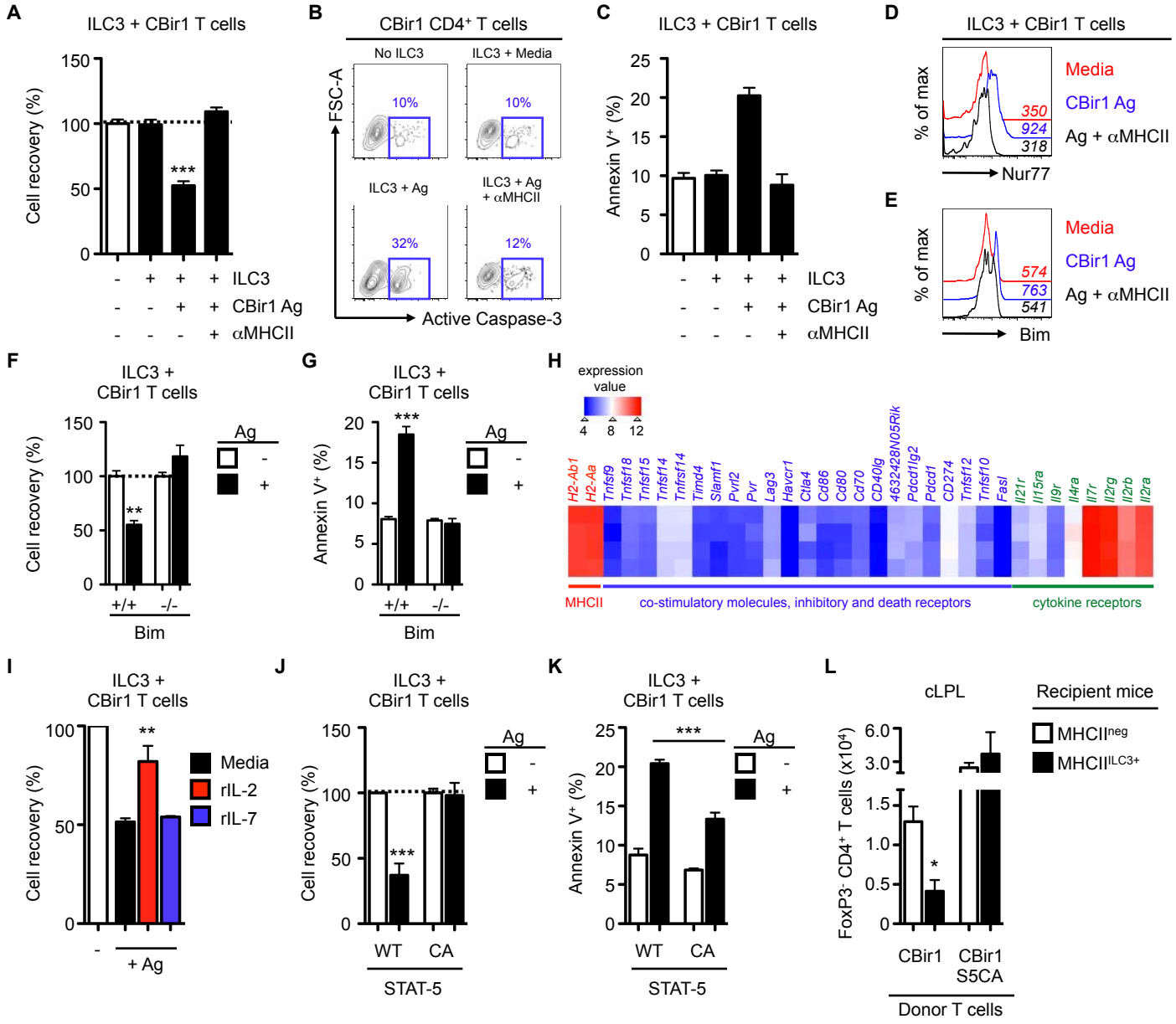
A
ILC3 + CBir1 T cells
Cell recovery (%)
150
100
50
0
***
- + + + ILC3
- - + + CBir1 Ag
- - - + αMHCII
B
CBir1 CD4+ T cells
No ILC3
ILC3 + Media
ILC3 + Ag
ILC3 + Ag + αMHCII
10%
10%
32%
12%
FSC-A
Active Caspase-3
C
ILC3 + CBir1 T cells
Annexin V+ (%)
25
20
15
10
5
0
- + + + ILC3
- - + + CBir1 Ag
- - - + αMHCII
D
ILC3 + CBir1 T cells
% of max
Media
CBir1 Ag
Ag + αMHCII
350
924
318
Nur77
E
% of max
Media
CBir1 Ag
Ag + αMHCII
574
763
541
Bim
F
ILC3 + CBir1 T cells
Cell recovery (%)
150
100
50
0
**
Ag
-
+
+/+
-/-
Bim
G
ILC3 + CBir1 T cells
Annexin V+ (%)
20
15
10
5
0
***
Ag
-
+
+/+
-/-
Bim
H
expression value
4
8
12
H2-Ab1
H2-Aa
Tnfsf9
Tnfsf18
Tnfsf15
Tnfsf14
Tnfsf14
Timd4
Slamf1
Pvrl2
Pvr
Lag3
Havcr1
Ctla4
Cd86
Cd80
Cd70
CD40lg
4632428N05Rik
Pdcd1lg2
Pdcd1
CD274
Tnfsf12
Tnfsf10
Fasl
Il21r
Il15ra
Il9r
Il4ra
Il7r
Il2rg
Il2rb
Il2ra
MHCII
co-stimulatory molecules, inhibitory and death receptors
cytokine receptors
I
ILC3 + CBir1 T cells
Cell recovery (%)
100
50
0
**
Media
rIL-2
rIL-7
-
+ Ag
J
ILC3 + CBir1 T cells
Cell recovery (%)
150
100
50
0
***
Ag
-
+
WT
CA
STAT-5
K
ILC3 + CBir1 T cells
Annexin V+ (%)
25
20
15
10
5
0
***
Ag
-
+
WT
CA
STAT-5
L
cLPL
Recipient mice
MHCIIneg
MHCIIILC3+
FoxP3- CD4+ T cells (x10^4)
6.0
3.0
1.5
1.0
0.5
0
*
CBir1
CBir1 S5CA
Donor T cells

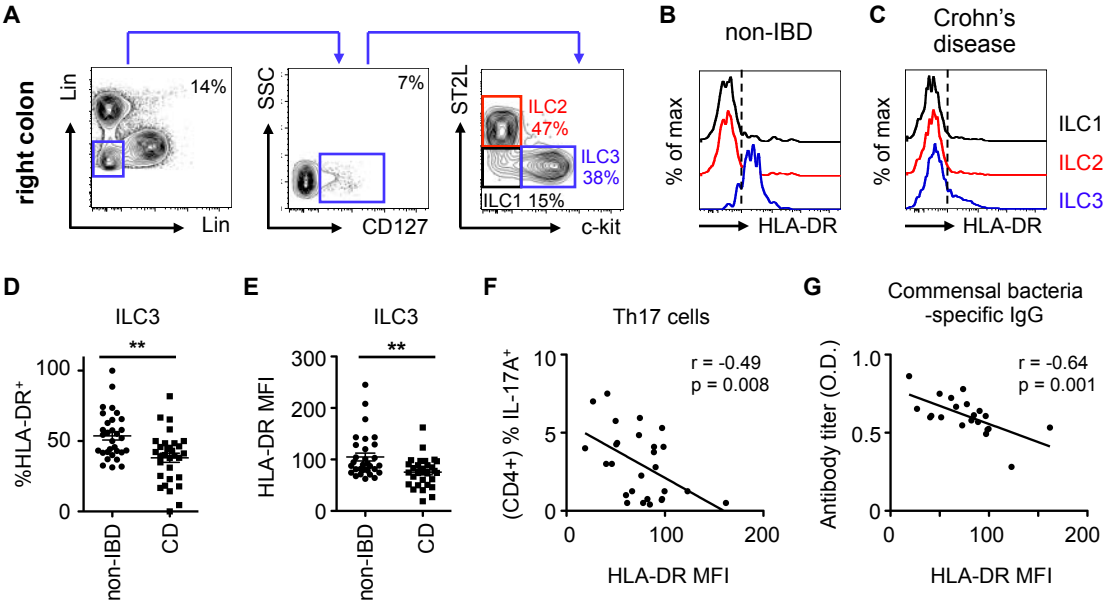
A
right colon
Lin
14%
Lin
SSC
7%
CD127
ST2L
ILC2
47%
ILC3
38%
ILC1 15%
c-kit
B
non-IBD
% of max
HLA-DR
C
Crohn's
disease
% of max
ILC1
ILC2
ILC3
HLA-DR
D
ILC3
**
%HLA-DR+
100
50
0
non-IBD
CD
E
ILC3
**
HLA-DR MFI
300
200
100
0
non-IBD
CD
F
Th17 cells
r = -0.49
p = 0.008
(CD4+) % IL-17A+
10
5
0
0
100
200
HLA-DR MFI
G
Commensal bacteria
-specific IgG
r = -0.64
p = 0.001
Antibody titer (O.D.)
1.0
0.5
0
0
100
200
HLA-DR MFI

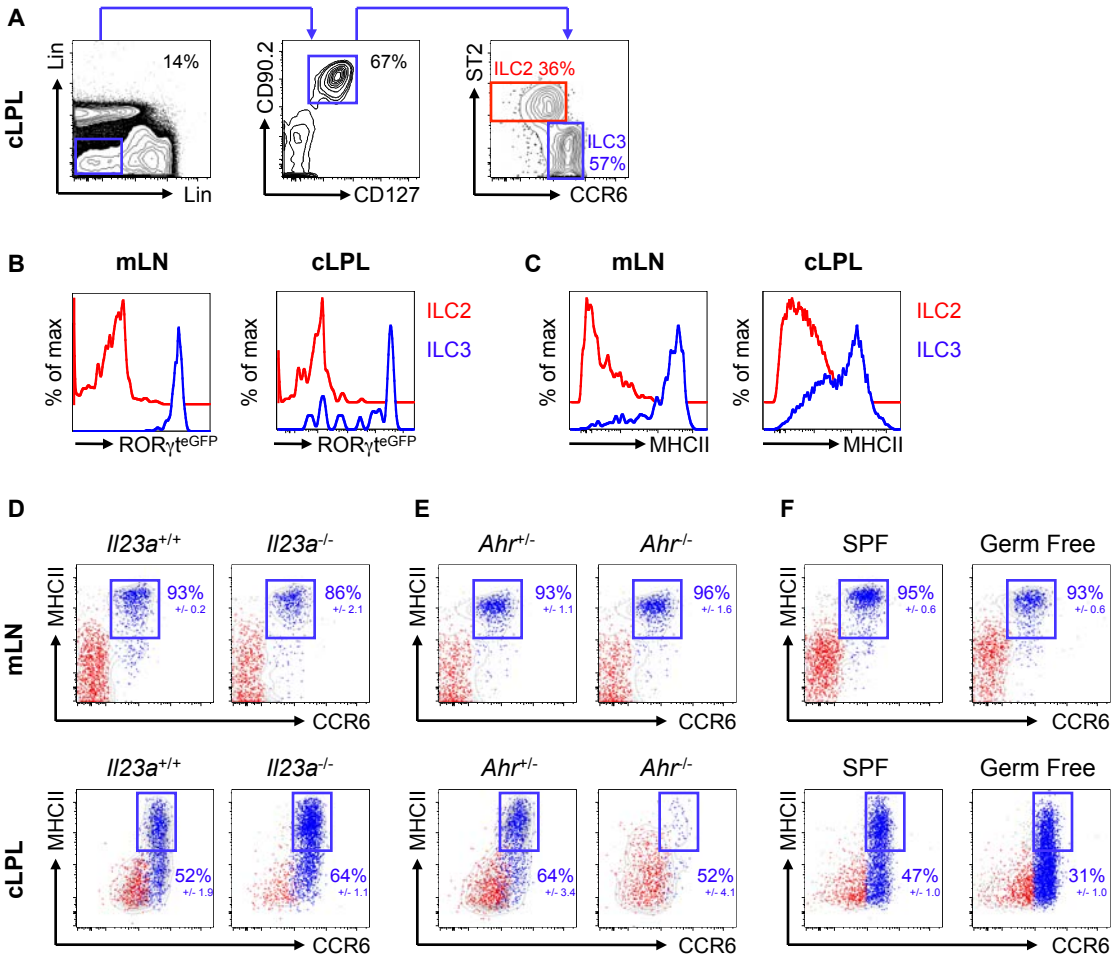
A
cLPL
Lin
14%
Lin
CD90.2
67%
CD127
ST2
ILC2 36%
ILC3
57%
CCR6
B
mLN
cLPL
% of max
RORγt^eGFP
ILC2
ILC3
C
mLN
cLPL
% of max
MHCII
ILC2
ILC3
D
Il23a+/+
Il23a-/-
mLN
cLPL
MHCII
CCR6
93% +/- 0.2
86% +/- 2.1
52% +/- 1.9
64% +/- 1.1
E
Ahr+/-
Ahr-/-
93% +/- 1.1
96% +/- 1.6
64% +/- 3.4
52% +/- 4.1
F
SPF
Germ Free
95% +/- 0.6
93% +/- 0.6
47% +/- 1.0
31% +/- 1.0

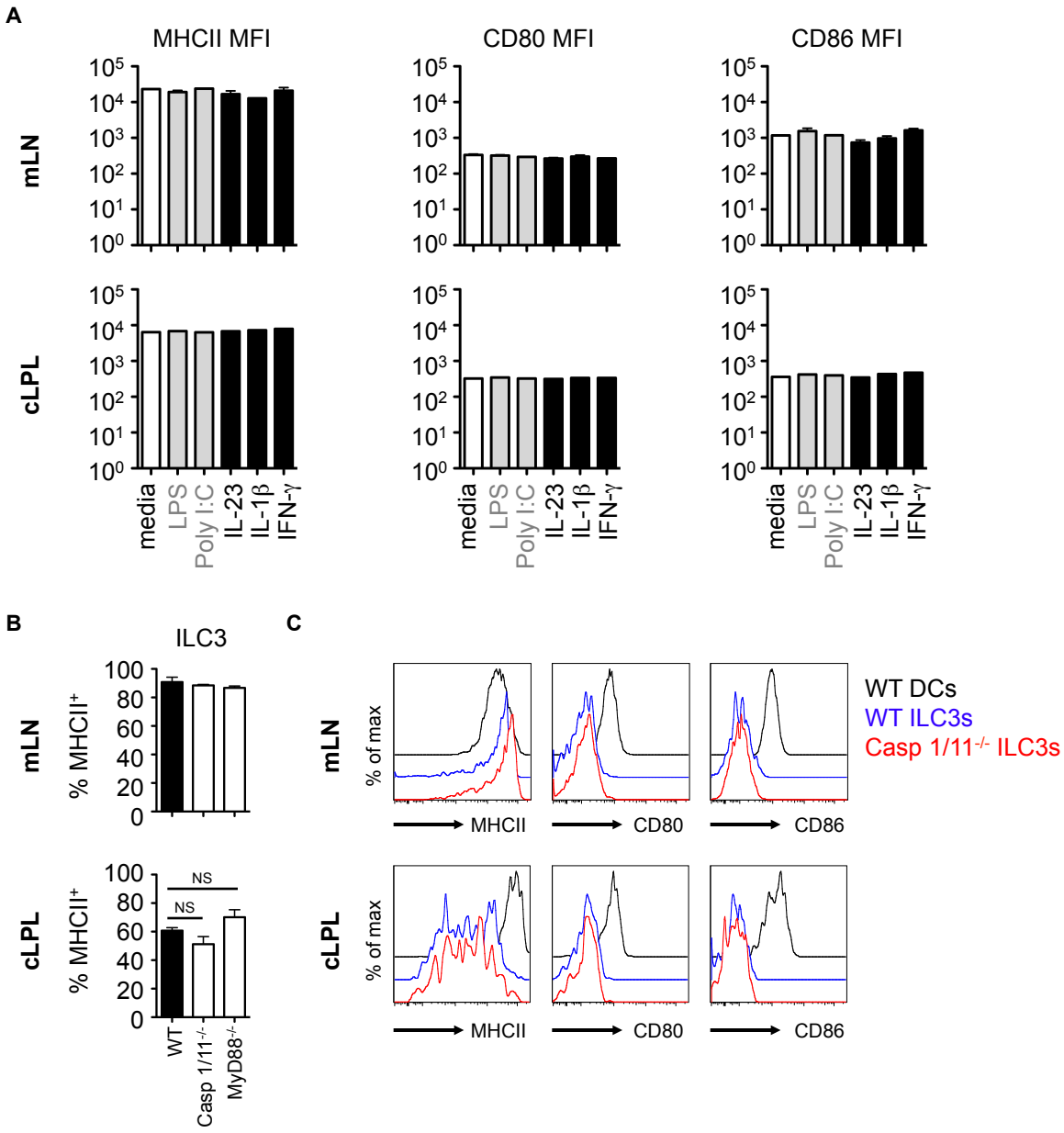
A
MHCII MFI
CD80 MFI
CD86 MFI
mLN
cLPL
media
LPS
Poly I:C
IL-23
IL-1β
IFN-γ
B
ILC3
% MHCII+
NS
WT
Casp 1/11-/-
MyD88-/-
C
% of max
MHCII
CD80
CD86
WT DCs
WT ILC3s
Casp 1/11-/- ILC3s

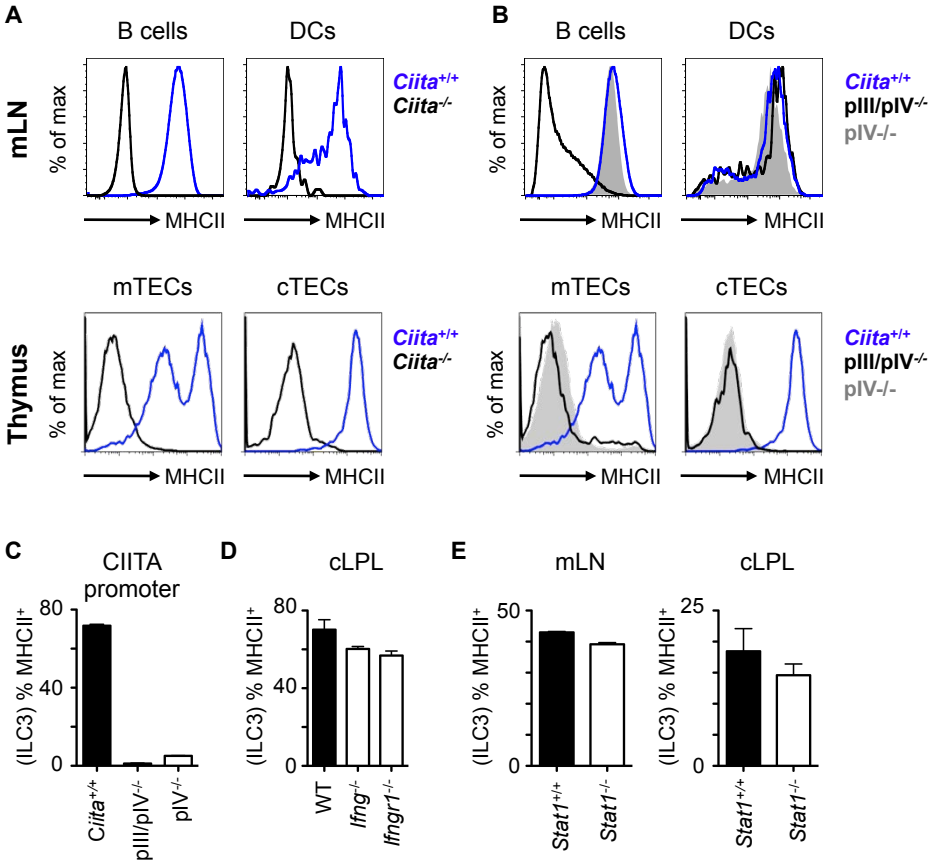
A
B cells
DCs
mLN
% of max
MHCII
Ciita+/+
Ciita-/-
B
pIII/pIV-/-
pIV-/-
mTECs
cTECs
Thymus
C
CIITA promoter
(ILC3) % MHCII+
80
40
0
Ciita+/+
pIII/pIV-/-
pIV-/-
D
cLPL
WT
Ifng-/-
Ifngr1-/-
E
mLN
50
Stat1+/+
Stat1-/-
25

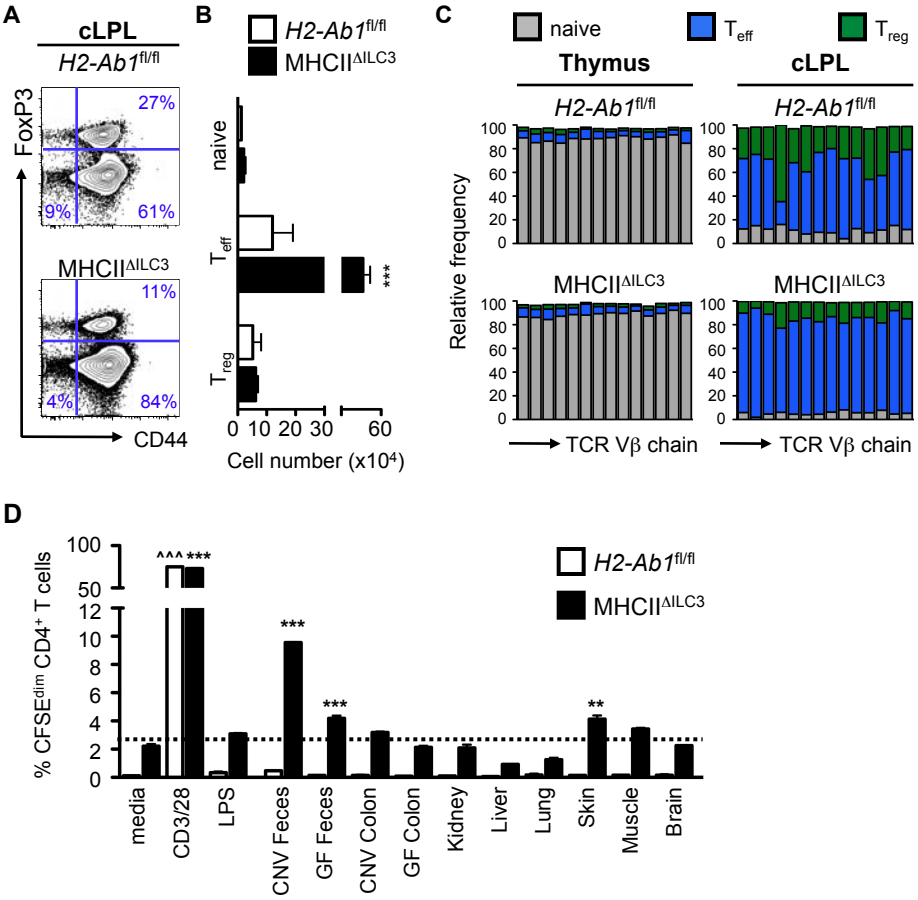
A
cLPL
H2-Ab1fl/fl
FoxP3
27%
9%
61%
MHCIIΔILC3
11%
4%
84%
CD44
B
H2-Ab1fl/fl
MHCIIΔILC3
naive
Teff
Treg
***
0 10 20 30 60
Cell number (x10⁴)
C
naive
Teff
Treg
Thymus
cLPL
H2-Ab1fl/fl
MHCIIΔILC3
Relative frequency
100
80
60
40
20
0
TCR Vβ chain
D
% CFSEdim CD4+ T cells
H2-Ab1fl/fl
MHCIIΔILC3
^^^***
***
***
**
media
CD3/28
LPS
CNV Feces
GF Feces
CNV Colon
GF Colon
Kidney
Liver
Lung
Skin
Muscle
Brain

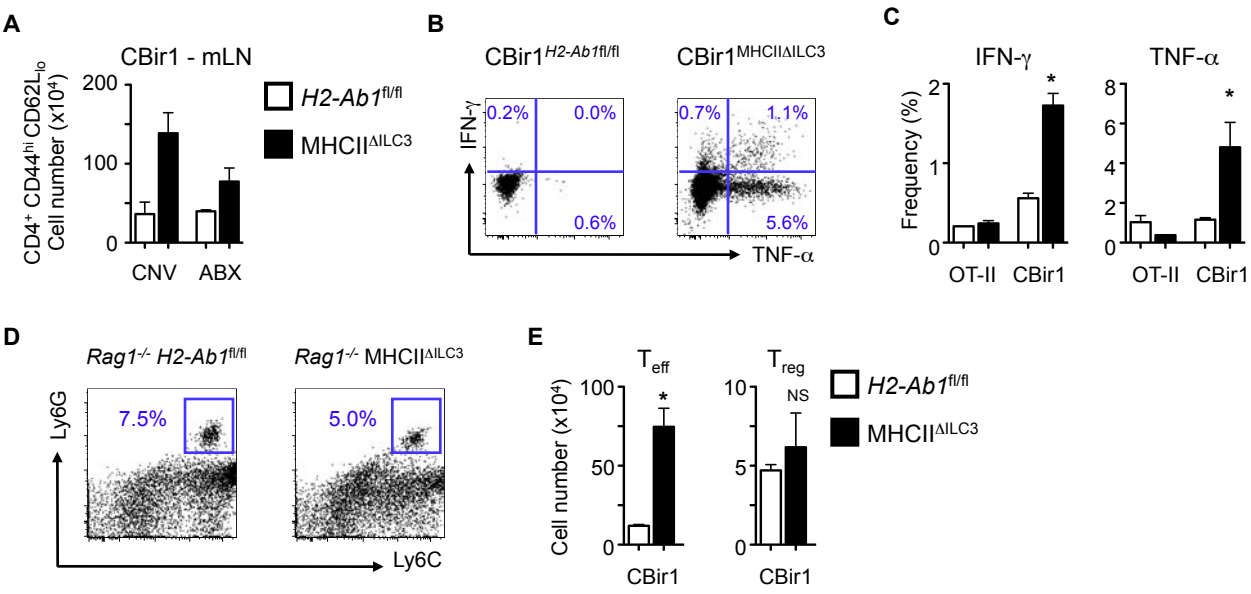
A
CBir1 - mLN
CD4+ CD44hi CD62Llo
Cell number (x10⁴)
200
100
0
CNV
ABX
H2-Ab1fl/fl
MHCIIΔILC3
B
CBir1H2-Ab1fl/fl
CBir1MHCIIΔILC3
IFN-γ
TNF-α
0.2%
0.0%
0.6%
0.7%
1.1%
5.6%
C
IFN-γ
TNF-α
Frequency (%)
OT-II
CBir1
D
Rag1-/- H2-Ab1fl/fl
Rag1-/- MHCIIΔILC3
Ly6G
Ly6C
7.5%
5.0%
E
Teff
Treg
Cell number (x10⁴)
NS
H2-Ab1fl/fl
MHCIIΔILC3

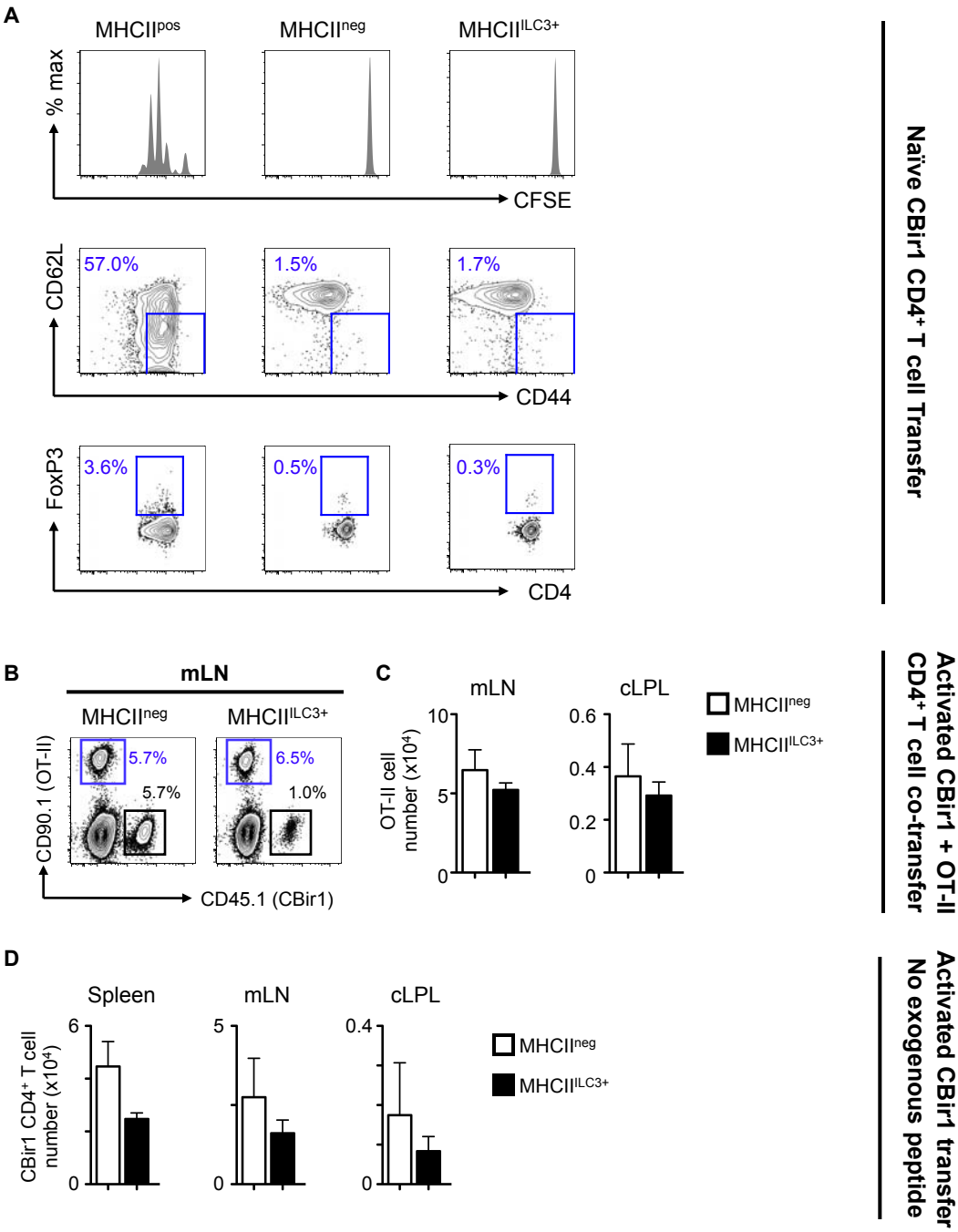
A
MHCIIpos
MHCIIneg
MHCIIILC3+
% max
CFSE
CD62L
57.0%
1.5%
1.7%
CD44
FoxP3
3.6%
0.5%
0.3%
CD4
Naïve CBir1 CD4+ T cell Transfer
B
mLN
MHCIIneg
MHCIIILC3+
CD90.1 (OT-II)
5.7%
5.7%
6.5%
1.0%
CD45.1 (CBir1)
C
mLN
cLPL
OT-II cell number (x10⁴)
10
5
0
0.6
0.4
0.2
0
MHCIIneg
MHCIIILC3+
Activated CBir1 + OT-II CD4+ T cell co-transfer
D
Spleen
mLN
cLPL
CBir1 CD4+ T cell number (x10⁴)
6
0
5
0
0.4
0
MHCIIneg
MHCIIILC3+
Activated CBir1 transfer No exogenous peptide

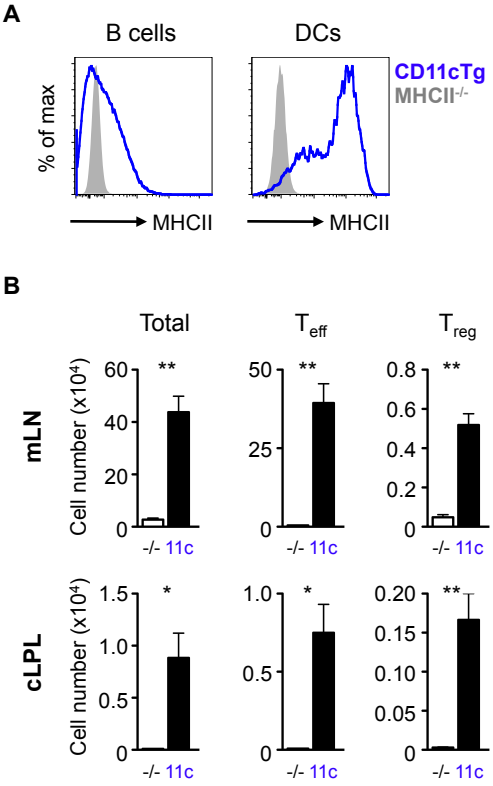
A
B cells
DCs
% of max
CD11cTg
MHCII-/-
MHCII
MHCII
B
Total
Teff
Treg
mLN
cLPL
Cell number (x10⁴)
-/- 11c
**
*

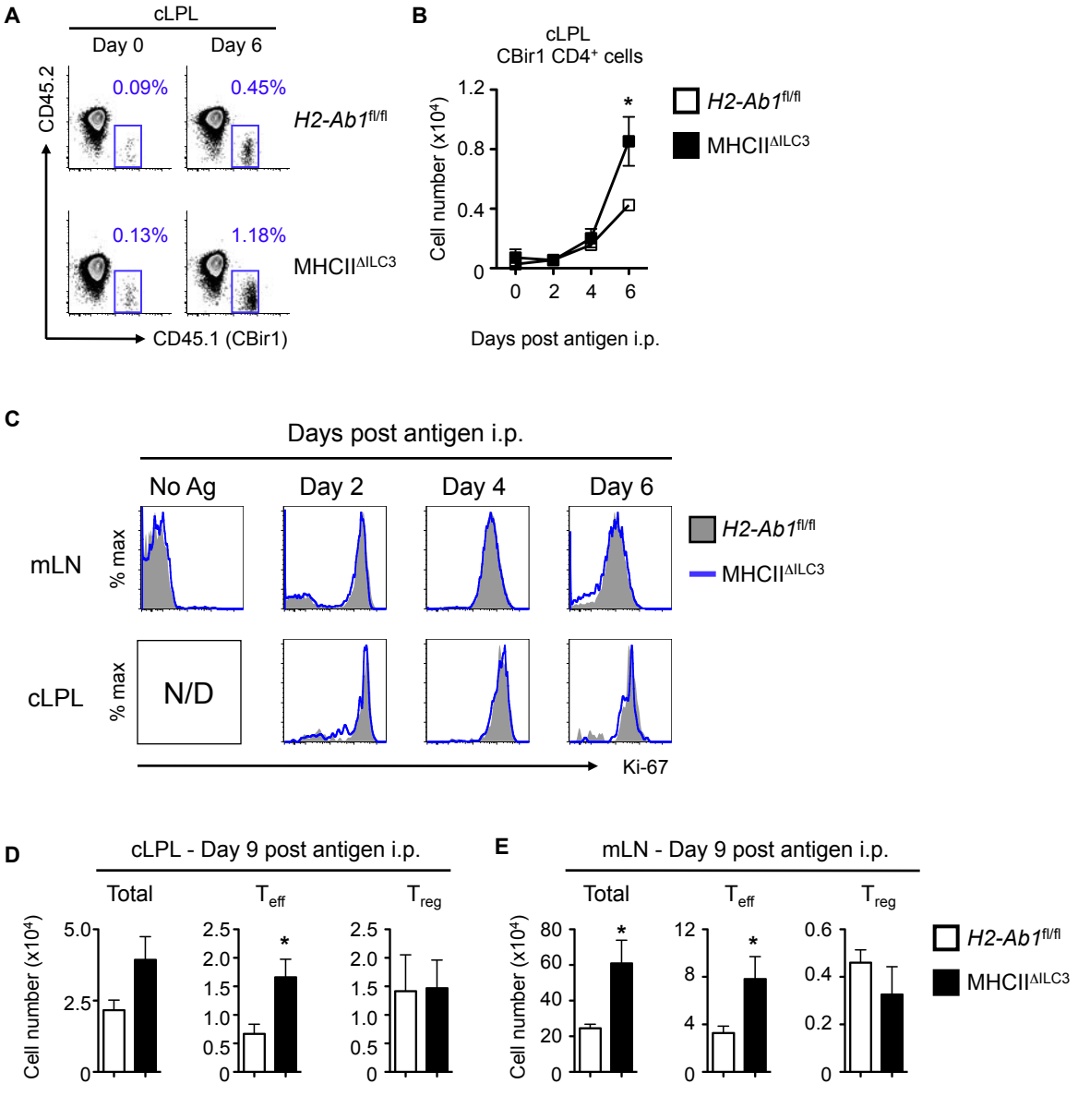
A
cLPL
Day 0
Day 6
CD45.2
0.09%
0.45%
H2-Ab1fl/fl
0.13%
1.18%
MHCIIΔILC3
CD45.1 (CBir1)
B
cLPL
CBir1 CD4+ cells
Cell number (x10⁴)
1.2
0.8
0.4
0
0 2 4 6
Days post antigen i.p.
H2-Ab1fl/fl
MHCIIΔILC3
C
Days post antigen i.p.
No Ag
Day 2
Day 4
Day 6
mLN
% max
cLPL
N/D
Ki-67
H2-Ab1fl/fl
MHCIIΔILC3
D
cLPL - Day 9 post antigen i.p.
Total
Teff
Treg
Cell number (x10⁴)
E
mLN - Day 9 post antigen i.p.
Total
Teff
Treg
Cell number (x10⁴)
H2-Ab1fl/fl
MHCIIΔILC3

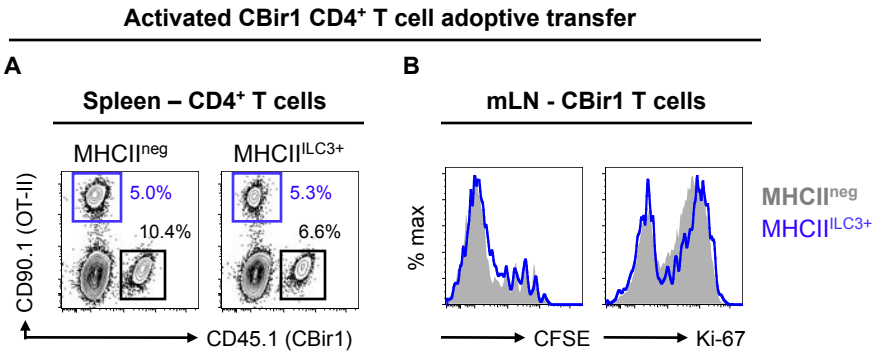
Activated CBir1 CD4+ T cell adoptive transfer
A
Spleen – CD4+ T cells
MHCIIneg
MHCIIILC3+
5.0%
10.4%
5.3%
6.6%
CD90.1 (OT-II)
CD45.1 (CBir1)
B
mLN - CBir1 T cells
% max
CFSE
Ki-67
MHCIIneg
MHCIIILC3+

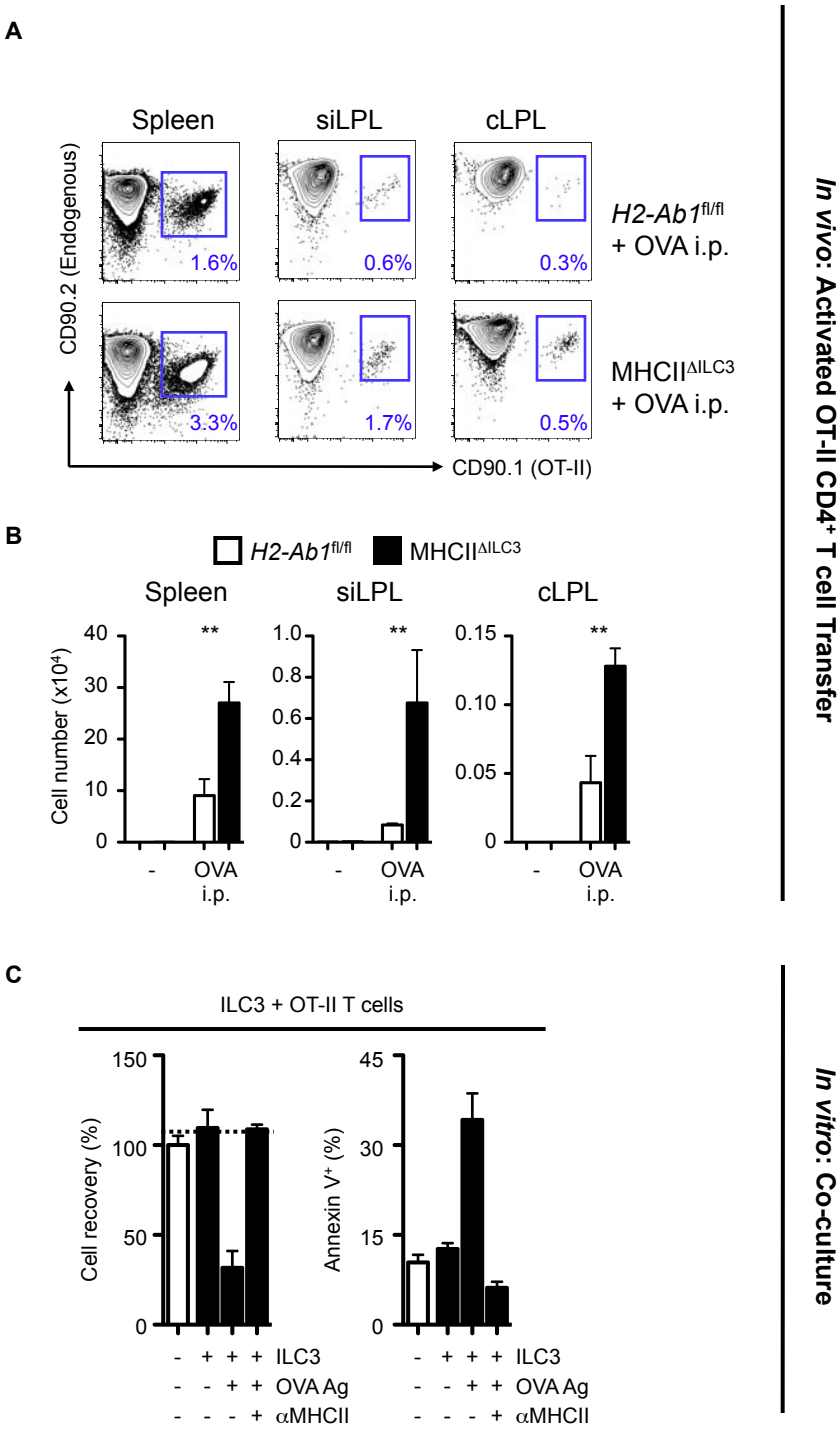
A
Spleen
siLPL
cLPL
CD90.2 (Endogenous)
1.6%
0.6%
0.3%
3.3%
1.7%
0.5%
CD90.1 (OT-II)
H2-Ab1fl/fl
+ OVA i.p.
MHCIIΔILC3
+ OVA i.p.
B
H2-Ab1fl/fl
MHCIIΔILC3
Spleen
siLPL
cLPL
Cell number (x10⁴)
**
- OVA i.p.
C
ILC3 + OT-II T cells
Cell recovery (%)
Annexin V⁺ (%)
ILC3
OVA Ag
αMHCII
In vivo: Activated OT-II CD4⁺ T cell Transfer
In vitro: Co-culture

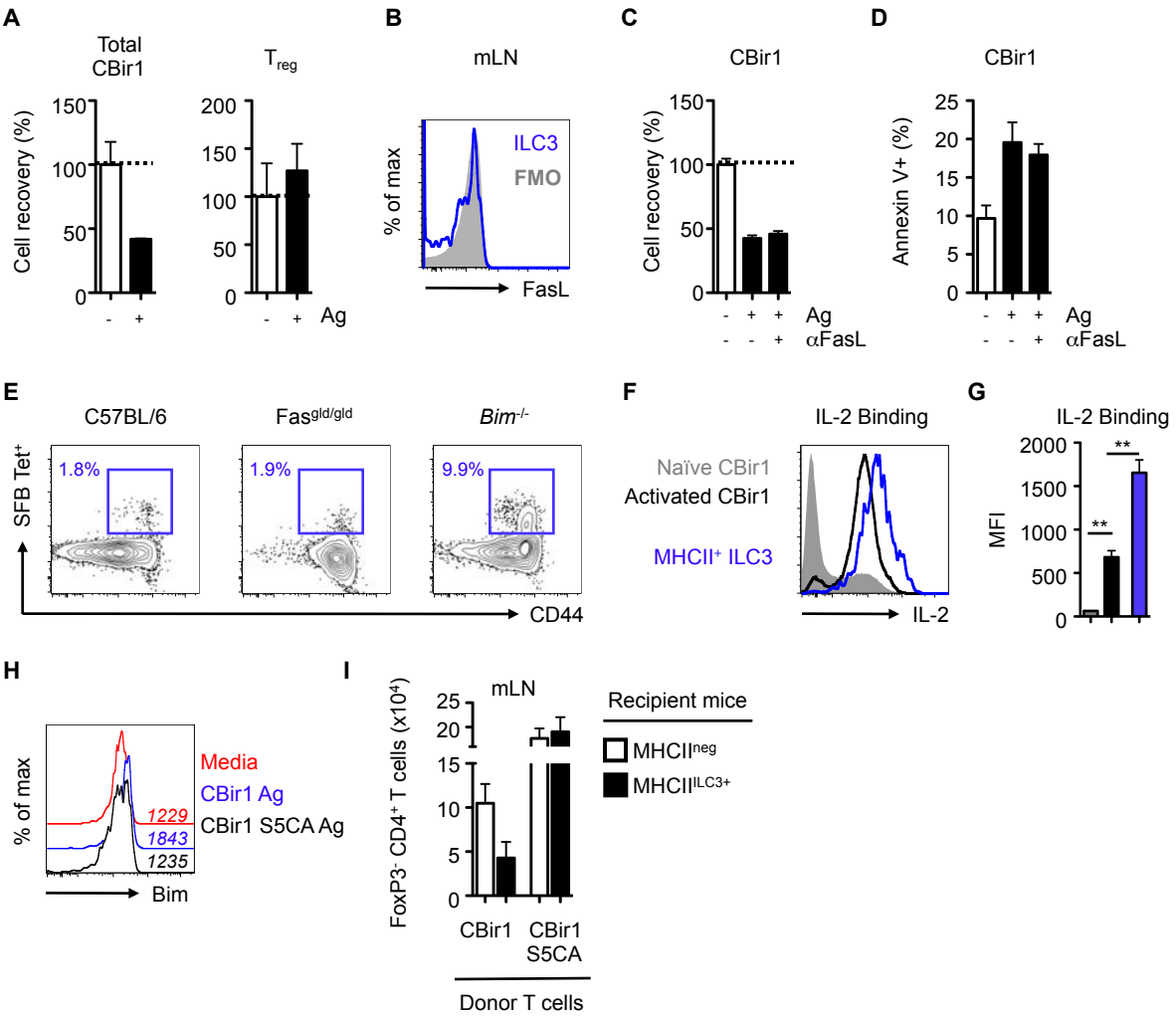
A
Total CBir1
T reg
Cell recovery (%)
150
100
50
0
200
150
100
50
0
- +
- + Ag
B
mLN
% of max
ILC3
FMO
FasL
C
CBir1
Cell recovery (%)
150
100
50
0
- + + Ag
- - + αFasL
D
CBir1
Annexin V+ (%)
25
20
15
10
5
0
- + + Ag
- - + αFasL
E
C57BL/6
Fasgld/gld
Bim-/-
SFB Tet+
1.8%
1.9%
9.9%
CD44
F
IL-2 Binding
Naïve CBir1
Activated CBir1
MHCII+ ILC3
IL-2
G
IL-2 Binding
MFI
2000
1500
1000
500
0
**
**
H
% of max
Media
CBir1 Ag
CBir1 S5CA Ag
1229
1843
1235
Bim
I
mLN
FoxP3- CD4+ T cells (x10^4)
25
20
15
10
5
0
CBir1
CBir1 S5CA
Donor T cells
Recipient mice
MHCIIneg
MHCIIILC3+

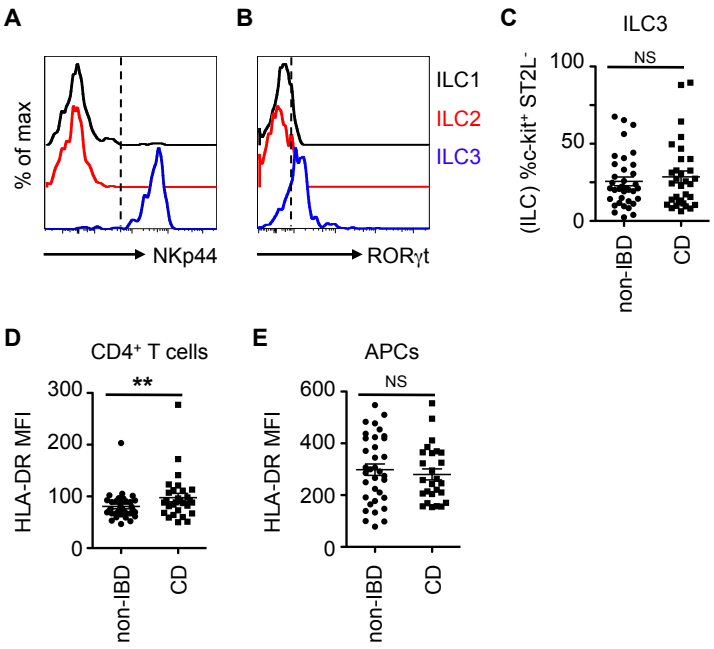
A
B
C
% of max
NKp44
RORγt
ILC1
ILC2
ILC3
ILC3
NS
100
50
0
(ILC) %c-kit+ ST2L-
non-IBD
CD
D
CD4+ T cells
**
300
200
100
0
HLA-DR MFI
non-IBD
CD
E
APCs
NS
600
400
200
0
HLA-DR MFI
non-IBD
CD

Fig. S13

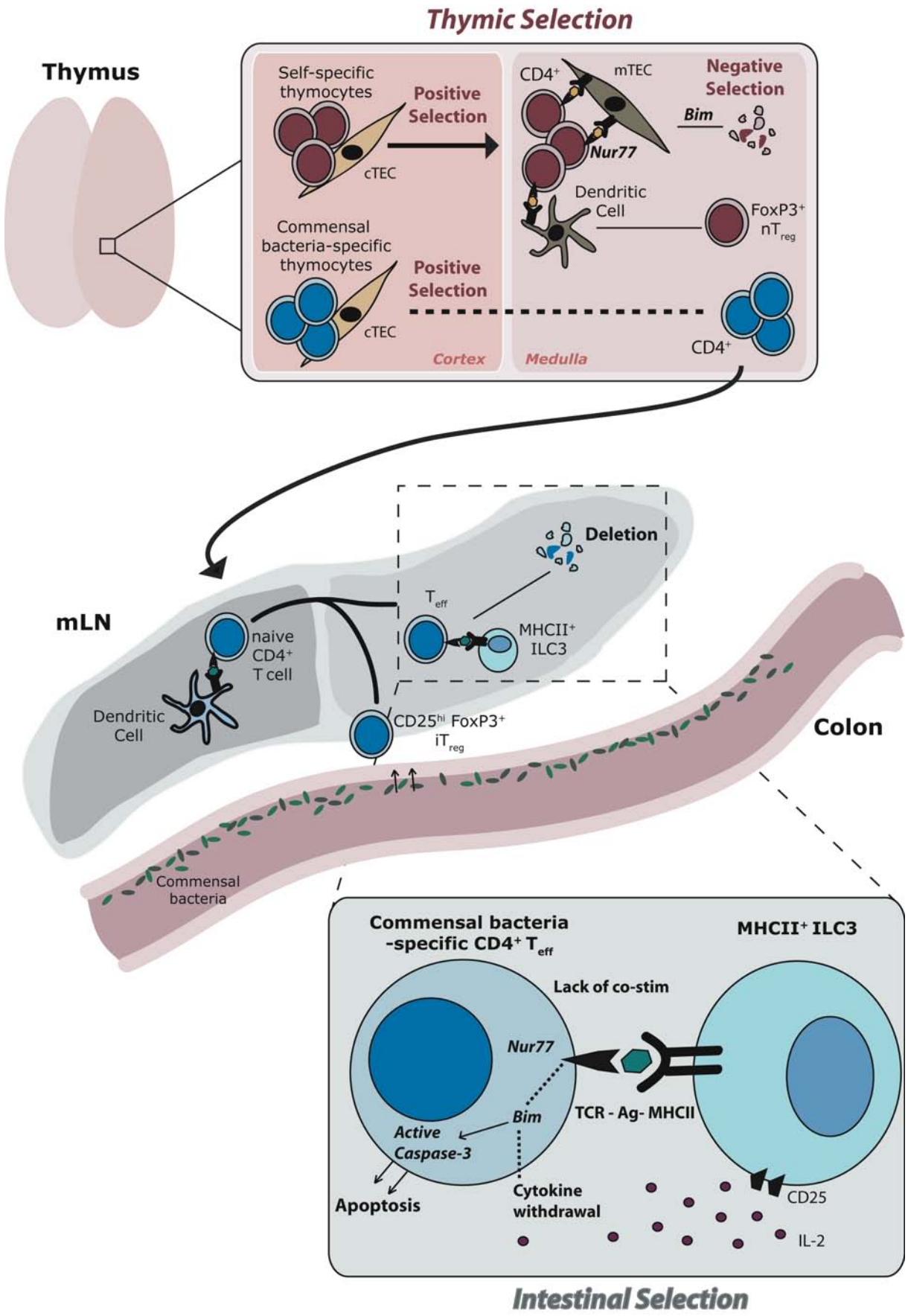
Thymic Selection
Thymus
Self-specific thymocytes
Positive Selection
cTEC
CD4+
mTEC
Negative Selection
Bim
Nur77
Dendritic Cell
FoxP3+ nTreg
Commensal bacteria-specific thymocytes
Positive Selection
cTEC
CD4+
Cortex
Medulla
Deletion
Teff
MHCII+ ILC3
mLN
naive CD4+ T cell
Dendritic Cell
CD25hi FoxP3+ iTreg
Colon
Commensal bacteria
Commensal bacteria -specific CD4+ Teff
MHCII+ ILC3
Lack of co-stim
Nur77
Bim
TCR - Ag- MHCII
Active Caspase-3
Apoptosis
Cytokine withdrawal
CD25
IL-2
Intestinal Selection

Supplementary Materials for

Group 3 innate lymphoid cells mediate intestinal selection of commensal bacteria-specific $CD4^+$ T cells

Matthew R. Hepworth, Thomas C. Fung, Samuel H. Masur, Judith R. Kelsen, Fiona M. McConnell, Juan Dubrot, David R. Withers, Stephanie Hugues, Michael A. Farrar, Walter Reith, Gerard Eberl, Robert N. Baldassano, Terri M. Laufer, Charles O. Elson, Gregory F. Sonnenberg

correspondence to: gfsonnenberg@med.cornell.edu

This PDF file includes:

Materials and Methods

Mice

Age- and sex-matched C57BL/6, OT-II, *Ciita*$^{-/-}$, *Ifng*$^{-/-}$, *Ifngr1*$^{-/-}$, *Bim*$^{-/-}$, *Fas*$^{gld/gld}$ and *Myd88*$^{-/-}$ mice were purchased from the Jackson Laboratory (Bar Harbor, ME) and *Stat1*$^{+/+}$ (129SvJ) and *Stat1*$^{-/-}$ mice were purchased from Taconic Farms. *Il23a*$^{-/-}$ mice were provided by Janssen Research and Development LLC and *Ahr*$^{-/-}$ mice were kindly provided by C. Hunter and S. Wagage (University of Pennsylvania). Caspase 1/11$^{-/-}$ were kindly provided by I. Brodsky (University of Pennsylvania). *Rorc(γt)-Gfp*^{TG} and *Rorc*^{Cre} mice were provided by G. Eberl (Institut Pasteur, Paris, France) and MHCII$^{\Delta ILC3}$ mice and *H2-Ab1*$^{fl/fl}$ littermate controls were generated as previously described (22). CD45.1^{+} CBir1 TCR transgenic mice were kindly provided by C. Elson (University of Alabama at Birmingham, USA) and crossed with MHCII$^{\Delta ILC3}$ mice to generate CBir1$^{MHCII\Delta ILC3}$ mice. CBir1 mice were also crossed with *Bim*$^{-/-}$ (Jackson Laboratory) or STAT-5 constitutively active mice (S5CA; kindly provided by M. Farrar, University of Minnesota) where indicated. IAβ^{b}STOP$^{fl/fl}$ mice (34), MHCII$^{-/-}$ and CD11cTg mice (42), were kindly provided by T. Laufer (University of Pennsylvania). All mice were maintained in specific pathogen-free facilities at Weill Cornell Medical College, New York and where appropriate mutant strains were co-housed with control littermates to ensure equivalent microbiota exposure. In some experiments, mice were administered a cocktail of broad-spectrum antibiotics in their drinking water *ad libitum* as previously described (22). Germ-free C57BL/6 mice were maintained at Weill Cornell Medical College, New York. *Ciita*$^{+/+}$ (C57BL/6), pIII/pIV$^{-/-}$ and pIV$^{-/-}$ mice were maintained at the University of Geneva, Switzerland and tissues were kindly provided by W. Reith and S. Hugues. All protocols were approved by the Weill Cornell Medical College Institutional Animal Care and Use Committees (IACUC), and all experiments were performed according to the guidelines of the relevant institution.

Transgenic CD4^{+} T cell adoptive transfers

In the majority of experiments, CBir1, CBir1 S5CA and/or OT-II CD4^{+} T cells were enriched using MACs negative selection column enrichment (Miltenyi Biotech) and activated for 18 h at 5x10^{6} cells/well in the presence of 0.5x10^{6} antigen-presenting cells and 1 μg/mL anti-CD3 and anti-CD28 monoclonal antibodies, prior to cell sorting on an Aria II (BD Biosciences). CD4^{+} T cells were then sort-purified to >98% purity and transferred into 6-10 week old recipient hosts as indicated. In some experiments naïve T cells were sort-purified to >98% purity and 5x10^{6} cells transferred without prior activation (naïve). Mice were then administered 50 μg CBir1$_{456-475}$ peptide or OVA$_{323-339}$ peptide i.p. every two days post-transfer as indicated. In some experiments T cells were further CFSE-labeled prior to transfer. Recipient mice were euthanized 9-10 days following transfer and the presence of TCR transgenic T cells was quantified in the mLN, small intestinal lamina propria and colonic lamina propria.

Murine tissue isolation and flow cytometry

Thymi and mLNs were harvested, and single-cell suspensions were prepared at necropsy. For intestinal lamina propria lymphocyte preparations, intestines were isolated, attached fat and Peyer's patches removed, and tissues cut open longitudinally. Luminal contents were removed by shaking in cold PBS. Epithelial cells and intra-epithelial lymphocytes were removed by shaking tissue in stripping buffer (1 mM EDTA, 1 mM DTT and 5% FCS) for 30 min at 37°C. The lamina propria layer was isolated by digesting the remaining tissue in 1.0 mg/mL collagenase/dispase (Roche) and 20 μg/mL DNase I (Sigma-Aldrich) for 30 min at 37°C. Thymic epithelial cells were stained in single-cell suspensions isolated from whole thymus by digestion in HBSS containing collagenase D (Roche) and DNase I (Sigma-Aldrich). Cell preparations were then depleted of $CD45^+$ cells using anti-CD45 magnetic beads and MACs column enrichment (Mitlenyi Biotec).

For flow cytometric analyses, cells were stained with antibodies to the following markers (all antibodies from eBioscience unless otherwise stated): anti-CD45.1 (clone M5/114.15.2), anti-Thy1.1 (clone H1551), anti-TCR Vβ5 (clone MR9.4, BD Biosciences), anti-TCR Vβ8.3 (clone 8C1, BioLegend), NK1.1 (clone PK136), anti-CD3 (clone 145-2C11), anti-CD5 (clone 53-7.3), anti-CD127 (clone A7R34), anti-CD90.2 (clone 30-H12, BioLegend) anti-CD11c (clone N418), anti-F4/80 (clone BM8), anti-Ly6C (clone HK1.4), anti-Ly6G (clone RB6-8C5), anti-CD4 (clone GK1.5), anti-CD8 (clone 53-6.7), anti-B220 (clone RA3-6B2), anti-CD25 (clone eBio3C7), anti-CD80 (clone 16-10A1), anti-CD86 (clone GL1) anti-MHCII (clone M5/114.15.2), anti-CD44 (clone IM7), anti-CD62L (clone MEL-14), anti-CD45 (clone 30-F11), anti-CD11b (clone M1/70), anti-CD117 (c-kit) (clone 2B8), anti-Nur77 (clone 12.14), anti-Bim (clone C34C5, Cell Signalling), anti-FasL (clone MFL3) anti-ST2 (IL-33R) (clone DJ8, MDbioproducts), anti-CCR6 (clone 29-2L17, BioLegend), anti-Ki-67 (clone B56, BD Biosciences), anti-EpCAM1 (clone G8.8, BioLegend) and anti-Ly5.1 (clone 6C3, BioLegend). For intracellular staining, cells were fixed and permeabilized utilizing a commercially available kit (eBioscience) and stained with anti-FoxP3 (clone FJK016s). For cytokine production, cells were stimulated *ex vivo* by incubation for 4 h with 50 ng/mL PMA, 750 ng/mL ionomycin, 10 μg/mL Brefeldin A (all obtained from Sigma-Aldrich) and permeabilized as indicated above and stained with anti-IFN-γ (clone XMG1.2) and anti-TNF-α (clone MP6-XT22). Dead cells were excluded from analysis using a violet viability stain (Invitrogen). T cell receptor Vβ chains were assessed using a commercial mouse TCR Vβ screening panel (BD Biosciences). SFB-specific $CD4^+$ T cell responses were measured in pooled gut-associated lymphoid tissues (mLN, Peyer's patches, siLPL and cLPL) using a specific MHCII-tetramer (IA^b/3340-A6), as previously described (31, 43). IL-2 binding capacity was assessed using a biotinylated IL-2 Fluorokine assay kit (R&D Systems), following manufacturer's instructions. Flow cytometry data collection was performed on an LSR II (BD Biosciences) and cell sorting was performed on an Aria II (BD Biosciences). Data were analyzed using FlowJo software (Tree Star Inc.).

In vitro ILC3-T cell co-culture assays

$Lineage^{neg}$ $CD127^+$ $CCR6^+$ ILC3s were sort-purified from the mLN of C57BL/6 mice and $5x10^3$ ILC3s were pulsed with 10 μg/mL CBir1 peptide, or OVA peptide where

indicated, in a 96-well plate for 1 h at 37°C/5% CO_2. Where indicated, antigen-pulsed ILC3s were further cultured in the presence of 1 μg/mL anti-MHCII (clone M5/114.15.2, eBioscience) or anti-FasL (clone MFL3, eBioscience). Whole mLN and splenic lymphocytes from CBir1 and OT-II mice were pre-activated with 10 μg/mL cognate antigen for 24 h prior to culture. Subsequently, T cells ($CD3^+$ $CD5^+$ $CD4^+$) were sort-purified and plated at $10x10^3$ cells per well in the presence or absence of ILC3s and co-cultured for 48 h. Prior to staining for flow cytometric analysis, cells were spiked with $1x10^6$ congenic (CD90.1) splenocytes to allow for reproducible recovery and analysis. Cell recovery was assessed using a known number of counting beads (AccuCheck, Molecular Probes). Cells were further assessed for apoptosis via quantification of active Caspase-3 (CaspGlow kit, eBioscience) or PE-Cy7 conjugated Annexin V (eBioscience).

In vitro stimulation assays

Lymphocyte preparations from naïve C57BL/6 mLN or cLPL were prepared as described above, $1x10^6$ cells/well plated in a 96-well plate in FCS-containing media and stimulated with media alone or 1 μg/mL LPS, 25 μg/mL Poly I:C, 100 ng/mL IL-23, 100 ng/mL IL-1β or 100 ng/mL IFN-γ for 48 h. MHCII and co-stimulatory molecules were then assessed by flow cytometry by gating on $CCR6^+$ ILC3. In other experiments, $CD4^+$ T cells were sort-purified from the spleen and mLN of $MHCII^{\Delta ILC3}$ mice and *H2-Ab1*$^{fl/fl}$ littermate controls, CFSE labeled, plated at a density of $2x10^6$ cells/well in a 24 well plate and stimulated with 50 μg/mL of fecal or tissue antigen preparations as indicated. Antigen preparations were generated by sterile dissection of peripheral tissues, with subsequent removal of colon and fecal content, and homogenized in PBS containing protease inhibitors and EDTA, followed by three rounds of sonication for 30 seconds at 50% amplitude. Debris was then pelleted by centrifugation at 12,000 x g, the soluble protein-containing supernatant was extracted and subjected to two freeze-thaw cycles and protein concentrations quantified using a Nanodrop 2000 (Thermo Scientific).

Human samples and flow cytometry

Human intestinal tissues from the right colon and left colon were obtained from the Children's Hospital of Philadelphia following an IRB-approved protocol. Single cell suspensions from intestinal tissues were obtained by incubating biopsies for 30 min at 37°C with shaking in stripping buffer (1 mM EDTA, 1 mM DTT and 5% FCS) to remove the epithelial layer. Supernatants were then discarded, and the lamina propria fraction was obtained by incubating the remaining tissue for 30 min at 37°C with shaking in digestion solution (0.5 mg/mL collagenase/dispase and 20 μg/mL DNase I). Remaining tissues were then mechanically dissociated and filtered through a 70 μm cell strainer. All cells were then viably cryopreserved in 90% FBS and 10% DMSO for side-by-side analysis at a later time point. Following thawing, cells were stained with antibodies to the following markers (all antibodies from eBioscience unless otherwise stated): anti-CD3 (clone UCHT1), anti-CD4 (clone OKT-4), anti-CD5 (clone UCHT2), anti-CD11b (clone M1/7B), anti-CD11c (clone 3.9), anti-CD14 (clone 61D3), anti-CD19 (clone 2H7), anti-HLA-DR (clone LN3), anti-CD127 (clone A019D5, Biolegend), anti-FcεRI (clone AER-37), anti-CD117 (c-kit) (clone 104D2), anti-ST2L (clone B4E6, MDbioproducts) and anti-NKp44 (clone Z231, BC Cytometry). For intracellular staining, cells were fixed and permeabilized utilizing a commercially available kit (eBioscience) and stained with

anti-IL-17A (clone eBio64DEC17) and anti-RORγt (clone AFKJS-9). Dead cells were excluded from analysis using a viability stain (Invitrogen). Flow cytometry data was collected using a LSR II (BD Biosciences). Data were analyzed using FlowJo software (Tree Star Inc.).

Immunofluorescence and histology

Sections of mLN were prepared and stained for RORγt and CD3 expression as previously described (44). Expression of MHCII was detected using anti-mouse I-A/I-E antibody conjugated to Alexa Fluor 647 (clone M5/114.15.2, Biolegend). Images were acquired with a Zeiss 780 Zen microscope and analyzed using Zen software (Zeiss). For histological analyses, sections of colon and other tissues were paraffin embedded, sectioned and stained with H&E as previously described (22). Images were acquired with a Nikon Eclipse TI microscope, using manufacturer's software.

Commensal bacteria-specific ELISA

Commensal bacterial antigen was generated as previously described (45). Briefly, colonic fecal contents from *Rag1*$^{-/-}$ mice were homogenized and centrifuged at 1,000 rpm to remove large aggregates, and the resulting homogenate was washed with sterile PBS twice by centrifuging for 1 min at 8,000 rpm. On the last wash, bacteria were resuspended in 2 mL ice-cold PBS and sonicated on ice. Samples were then centrifuged at 20,000 x g for 10 min, and supernatants were recovered for a crude commensal bacteria antigen preparation. For measurement of serum antibodies by ELISA, 5 μg/mL commensal bacteria antigen was coated on 96-well plates, and sera were incubated in doubling dilutions. Antigen specific IgG was detected using an anti-human IgG-HRP antibody (BD Biosciences). Plates were developed with TMB peroxidase substrate (KPL), and optical densities were measured using a plate spectrophotometer.

Microarray

CCR6^{+} ILC3s were sort-purified from mLN by gating on lineage-negative, CD127^{+}, CD25^{+}, ST2^{-}, CCR6^{+} cells. RNA purification and arrays were performed as previously described (46). Microarray gene expression data was deposited at GEO (accession number GSE67076).

Statistical analyses

Results represent mean +/- s.e.m. Statistical analyses were performed by Student's t-test or one-way ANOVA unless specified otherwise.

Fig. S1.

fig. S1. MHCII expression of mLN and cLPL group 3 ILCs is independent of IL-23, Ahr and the intestinal microbiota. A) Colonic lamina propria cells from naïve mice were gated as $CD45^+$ and lineage (x-axis; CD3, CD5, CD8, NK1.1, y-axis; B220, CD11c, CD11b) negative and $CD127^+$ and further divided by expression of ST2 (ILC2s; red) or CCR6 (ILC3s; blue) and expression of **B)** $ROR\gamma t^{eGFP}$ or **C)** MHC class II was determined on mLN and cLPL ILC3s. Expression of MHCII on ILC2s (red) and ILC3s (blue) in mice deficient in **D)** IL-23p19 **E)** Aryl hydrocarbon receptor (Ahr) or **F)** intestinal microbiota from the mLN (top panel) and cLPL (bottom panel). Gate shows frequency of MHCII expression amongst gated ILC3s (blue). All data representative of at least 3 independent experiments with at least n=3 mice per group. SPF, specific pathogen free. Results are shown as the mean +/- s.e.m.

Fig. S2.

fig. S2. MHCII and co-stimulatory molecule expression of mLN ILC3s is unaffected by TLR ligands or pro-inflammatory cytokines. A) Mean fluorescent intensity of ILC3 MHCII, CD80 and CD86 from mLN or cLPL cells stimulated with media alone, TLR ligands (LPS, Poly I:C) or pro-inflammatory cytokines (IL-23, IL-1β, IFN-γ). **B)** Frequency of $MHCII^{+}$ (Lin^{-} $CD127^{+}$ $CCR6^{+}$) ILC3s in the mLN (top panel) and cLPL (bottom panel) of Capase $1/11^{-/-}$ and $MyD88^{-/-}$ mice. **C)** Representative histograms depicting expression of MHCII, CD80 and CD86 on WT C57BL/6 DCs (black line), WT ILC3s (blue line) or Capase $1/11^{-/-}$ ILC3s (red line) in the mLN (top panel) or cLPL (bottom panel). All data representative of at least 3 independent experiments with 3-4 mice per group or 3 biological replicates. Results are shown as the mean +/- s.e.m.

Fig. S3.

fig. S3. CIITA transcriptional control of MHCII expression on B cells, DCs and TECs and IFN-γ dependence of MHCII expression in colonic ILC3s. Expression of MHCII was determined on $B220^{+}$ $CD11c^{-}$ B cells or $CD11b^{+}$ $CD11c^{hi}$ DCs from the mLN or $CD45^{-}$ $EpCAM^{+}$ $Ly51^{-/low}$ mTECs or $CD45^{-}$ $EpCAM^{+}$ $Ly51^{+}$ cTECs from the thymus of mice deficient in **A)** CIITA and **B)** CIITA-specific promoters (pIII/pIV, pIV). MHCII expression on **C)** mLN $CCR6^{+}$ ILC3s from mice deficient CIITA in promoter regions (pIII/pIV, pIV) **D)** cLPL $CCR6^{+}$ ILC3s from IFN-γ or IFN-γR1-deficient mice and E) mLN and cLPL $CCR6^{+}$ ILC3s from STAT-1 deficient mice. All data representative of at least 3 independent experiments with n=2-3 mice per group. Results are shown as the mean +/- s.e.m.

Fig. S4.

fig. S4. ILC3-intrinsic MHCII selectively controls commensal bacteria-specific CD4$^+$ T effector cells in the intestine. A) Relative frequencies and **B)** total cell numbers of naïve (CD44^{lo}), T_{eff} (CD44^{hi}) and T_{reg} (FoxP3$^+$) CD4$^+$ T cells in the colonic lamina propria of MHCII$^{\Delta ILC3}$ mice or H2-Ab1$^{fl/fl}$ littermate controls. **C)** Analysis of the frequencies of naïve (grey), T_{eff} (blue) and T_{reg} (green) amongst CD4$^+$ T cells expressing commonly utilized TCR Vβ chains in the thymus and colonic lamina propria of MHCII$^{\Delta ILC3}$ mice or H2-Ab1$^{fl/fl}$ littermate controls. **D)** Frequency of proliferating cells (CFSE^{dim}) in CD4$^+$ T cells derived from MHCII$^{\Delta ILC3}$ mice or H2-Ab1$^{fl/fl}$ littermate controls and stimulated with fecal and tissue-derived homogenate antigens in vitro for 72 h. All data representative of at least 2 independent experiments with 3 biological replicates or n=3 mice per group. Results are shown as the mean +/- s.e.m. Data was analyzed by student's t-test (B) or one-way ANOVA (D). ** $p \leq 0.01$ and *** $p \leq 0.001$, ^^^ indicates $p \leq 0.001$ for H2-Ab1$^{fl/fl}$ comparisons versus matched media control.

Fig. S5.

fig. S5. ILC3-intrinsic MHCII selectively controls CBir1 CD4$^+$ T effector cells in the intestine. OT-II or CBir1 TCR transgenic mice were crossed with either MHCII$^{\Delta ILC3}$ mice or H2-Ab1$^{fl/fl}$ littermate controls and total Vβ5$^+$ (OT-II) or Vβ8.3$^+$ (CBir1) CD4$^+$ T cell numbers were determined. **A)** CBir1 CD4$^+$ T cell numbers in the mLN of conventional or ABX-treated CBir1 transgenic mice crossed with either MHCII$^{\Delta ILC3}$ mice or H2-Ab1$^{fl/fl}$ littermate controls. **B-C)** Frequencies of IFN-γ^+ and/or TNF-α^+ T cells following stimulation with cognate antigen, OVA peptide (OT-II) or CBir1 peptide (CBir1), for 5 h in the presence of Brefeldin A. **D)** Frequencies of CD45$^+$ CD3$^-$ B220$^-$ Ly6C$^+$ Ly6G$^+$ neutrophils in the cLPL of Rag1$^{-/-}$ MHCII$^{\Delta ILC3}$ mice or Rag1$^{-/-}$ H2-Ab1$^{fl/fl}$ littermate controls. **E)** Number of CD4$^+$ T_{eff} or T_{reg} in the colonic lamina propria of CBir1 transgenic mice crossed with either MHCII$^{\Delta ILC3}$ mice or H2-Ab1$^{fl/fl}$ littermate controls. All data representative of at least 3 independent experiments with n=2-3 mice per group. Results are shown as the mean +/- s.e.m. * $p < 0.05$, ** $p < 0.01$, *** $p < 0.001$ (two-tailed students t-test).

Fig. S6.

fig. S6. ILC3-restricted MHCII expression is not sufficient to induce proliferation, activation or T_{reg} differentiation of naïve CBir1 $CD4^+$ T cells, but induces antigen-specific deletion of activated T cells in vivo. A) $MHCII^{pos}$, $MHCII^{neg}$ and $MHCII^{ILC3+}$ mice received sort-purified naive CFSE-labeled $CD45.1^+$ CBir1 $CD4^+$ T cells and were injected with CBir1 peptide i.p. and analyzed for proliferation (CFSE dilution; upper panel) and frequencies of $CD4^+$ $CD45.1^+$ $CD44^{hi}CD62L^{lo}$ effector T cells (T_{eff}; middle panel) or $CD4^+$ $CD45.1^+$ $FoxP3^+$ regulatory T cells (T_{reg}; lower panel) in the mLN. **B)** Frequencies and **C)** numbers of activated congenic $CD90.1^+$ OT-II and $CD45.1^+$ Cbir1 T cells transferred at a 1:1 ratio in the mLN and cLPL of recipient $MHCII^{neg}$ or $MHCII^{ILC3+}$ mice which received CBir1 peptide. **D)** Cell numbers of transferred CBir1 T cells in the spleen, mLN and cLPL of recipient $MHCII^{neg}$ or $MHCII^{ILC3+}$ mice one month post-transfer in the absence of exogenously administered CBir1 peptide. All data representative of at least 3 independent experiments with n=2-3 mice per group. Results are shown as the mean +/- s.e.m.

Fig. S7.

fig. S7. $CD11c^+$ DC-restricted expression of MHCII drives expansion of commensal bacteria-specific T_{eff} and T_{reg}. A) Expression of MHCII on $B220^+$ B cells or $CD11c^+$ DCs in the mLN of CD11c transgenic (CD11cTg) mice (blue line) and $MHCII^{-/-}$ mice (grey fill). B) Numbers of total $CD45.1^+$ CBir1 $CD4^+$ T cells, $CD44^+$ $CD62L^{lo}$ (T_{eff}) CBir1 $CD4^+$ T cells and $FoxP3^+$ CBir1 $CD4^+$ T_{reg} cells in the mLN (top panel) and cLPL (bottom panel) of CD11cTg mice or $MHCII^{-/-}$ mice. All data representative of 2 independent experiments with n=3 mice per group. Results are shown as the mean +/- s.e.m. * $p < 0.05$, ** $p < 0.01$ (two-tailed students t-test).

Fig. S8.

fig. S8. ILC3-intrinsic deletion of MHCII results in selective expansion of CD4$^+$ CBir1 effector T cells in the intestine and associated lymphoid tissue. (A-C) MHCII$^{\Delta ILC3}$ mice and *H2-Ab1*$^{fl/fl}$ littermate controls received CD45.1$^+$ CBir1 Tg CD4$^+$ T cells that had been sort-purified following pre-activation and were injected with CBir1 peptide i.p. on day 0 and day 1 post transfer. **A)** Frequencies, **B)** numbers and **C)** proliferation (Ki-67) of transferred CBir1 T cells were quantified 0-6 days following antigen administration in the mLN and cLPL. **(D-E)** MHCII$^{\Delta ILC3}$ mice and *H2-Ab1*$^{fl/fl}$ littermate controls received CD45.1$^+$ CBir1 Tg CD4$^+$ T cells that had been sort-purified following pre-activation and were injected with CBir1 peptide i.p. every 2 days post transfer. Frequencies and numbers of total transferred CD4$^+$ CD45.1$^+$ T cells, CD4$^+$ CD45.1$^+$ CD44^{hi} CD62L^{lo} effector T cells (T_{eff}) or CD4$^+$ CD45.1$^+$ FoxP3$^+$ regulatory T cells (T_{reg}) were analyzed in **D)** the colonic lamina propria (cLPL) and **E)** the mLN. All data representative of at least 3 independent experiments with n=2-3 mice per group. N/D = not detected. Results are shown as the mean +/- s.e.m. * $p < 0.05$ (two-tailed students t-test).

Fig. S9.

fig. S9. MHCII^{+} ILC3 control of commensal bacteria-specific CD4^{+} T cells is not mediated via altered homing or suppression of proliferation. A) Frequencies of adoptively transferred activated CD45.1^{+} CBir1 and CD90.1^{+} OT-II CD4^{+} T cells in the spleen of MHCII^{neg} and MHCII^{ILC3+} mice administered CBir1 antigen at day 9 post transfer. **B)** CFSE dilution and Ki-67 expression of transferred activated CD45.1^{+} CBir1 CD4^{+} T cells in the mLN of MHCII^{neg} (grey fill) or MHCII^{ILC3+} mice (blue line) at day 9 post transfer. Data are representative of at least 2 independent experiments with n=3 mice per group.

Fig. S10.

fig. S10. MHCII^{+} ILC3s may also control expansion of non-commensal bacteria-specific T cells upon systemic administration of exogenous cognate antigen. A) Frequencies of congenic CD90.1^{+} OT-II cells in the mLN of recipient mice that received OVA peptide i.p. every 2 days following transfer. **B)** Total numbers of OT-II T cells in the mLN, siLPL and cLPL of recipient mice. **C)** Relative cell recovery (%) and frequency of Annexin V^{+} cells during *in vitro* co-culture of OT-II T cells and antigen-pulsed ILC3s in the presence or absence of an anti-MHCII neutralizing antibody. Data are representative of 2 independent experiments with 3 mice per group (A-B) or 2 independent experiments with 2-3 biological replicates per group (C). Results are shown as the mean +/- s.e.m. ** $p < 0.01$ (two-tailed students t-test).

Fig. S11.

fig. S11. MHCII^{+} ILC3s induce apoptotic cell death in CBir1 CD4^{+} T cells. A) Activated CBir1 CD4^{+} T cells were co-cultured with ILC3s in the presence or absence of CBir1 antigen and relative cell recovery (%) of either total CD45.1^{+} CBir1 CD4^{+} T cells or FoxP3^{+} CBir1 T_{reg} cells were quantified after 48 hours. **B)** Expression of FasL by CCR6^{+} ILC3s and **C)** relative cell recovery (%) and **D)** frequency of Annexin V^{+} cells during *in vitro* co-culture of CBir1 T cells and ILC3s in the presence or absence of anti-FasL neutralizing antibody. **E)** mLN, PP, siLPL and cLPL lymphocytes (GALT) were pooled and labeled with an SFB-specific MHCII tetramer and frequencies of SFB-specific CD4^{+} T cells quantified in C57BL/6, Fas$^{gld/gld}$ or *Bim*$^{-/-}$ mice. **F)** Representative histograms demonstrating IL-2 binding capacity and **G)** quantification of bound IL-2 MFI of naïve CBir1 CD4^{+} T cells (grey), antigen-activated CBir1 CD4^{+} T cells (black) and CCR6^{+} MHCII^{+} ILC3s (blue). **H)** Expression of Bim by wild type CBir1 CD4^{+} T cells or CBir1 CD4^{+} T cells with a constitutively active STAT-5 signaling molecule following co-culture with Ag-pulsed MHCII^{+} ILC3. **I)** Wild type CBir1 CD4^{+} T cells or CBir1 STAT5-CA CD4^{+} T cells were adoptively transferred into MHCII^{neg} or MHCII^{ILC3+} mice. Mice were administered CBir1 antigen and numbers of FoxP3^{-} CD45.1^{+} CBir1 T cells in the mLN were quantified 9 days post transfer. *In vitro* data representative of at least 2 independent experiments with 2-3 biological replicates per culture condition, *in vivo* data representative of at least 2 independent experiments with 3 mice per group. Results are shown as the mean +/- s.e.m. ** $p < 0.01$ (two-tailed students t-test).

Fig. S12.

fig. S12. ILC3 phenotype and frequencies in the intestine of non-IBD and pediatric Crohn's disease patients. ILC subsets as gated in Fig. 4A were analyzed for expression of the human ILC3 markers **A)** NKp44 and **B)** RORγt. **C)** Frequencies of c-kit^{+} ST2L^{-} ILC3s within the Lin^{neg} CD127^{+} ILC gate were analyzed in right colon biopsies from pediatric Crohn's disease (CD) and non-IBD controls. **(D-E)** HLA-DR expression (MFI) was quantified on **D)** CD4^{+} T cells or **E)** CD19^{+} CD11c^{+} APCs in the same cohort of non-IBD or Crohn's disease patients as depicted in Figure 4. Results are shown as the mean +/- s.e.m. Statistical analyses between patient groups are performed using a Mann-Whitney test * $p < 0.05$, ** $p < 0.01$, *** $p < 0.001$.

Fig. S13.

fig. S13. Intestinal selection of commensal bacteria-specific CD4$^+$ T cells. Thymocytes with specificity for either self or commensal bacteria undergo positive selection through interactions with cortical thymic epithelial cells (cTECs), subsequently differentiate into mature CD4$^+$ T cells and migrate into the thymic medulla. Once in the medulla self-specific CD4$^+$ T cells are subject to negative selection through interactions with MHCII$^+$ medullary thymic epithelial cells (mTECs) and dendritic cells presenting self-antigen. This process of negative selection is mediated by programmed cell death, associated with Nur77 signaling and Bim-dependent apoptosis, which results in the deletion of self antigen-specific CD4$^+$ T cells prior to entering the periphery. In contrast, CD4$^+$ T cells specific for commensal bacteria fail to undergo negative selection due to the absence of commensal bacteria-derived antigen in the thymus. Rather, mature commensal bacteria-specific CD4$^+$ T cells enter the peripheral circulation where they may encounter professional antigen-presenting cells, such as dendritic cells, presenting commensal bacteria-derived antigen via MHCII. Antigen-experienced T_{eff} then migrate to distinct niches within the lymph node, which are enriched for MHCII$^+$ ILC3s, resulting in the deletion of activated commensal bacteria-specific T_{eff} cells from the peripheral pool. Commensal bacteria-specific T cells receive TCR signals from ILC3 MHCII-Ag complexes in the absence of co-stimulation, which is associated with upregulation of the signaling molecule Nur77. In addition, ILC3s efficiently consume growth factor cytokines, in particular IL-2, resulting in T cell cytokine withdrawal. The net effect of both TCR signaling and cytokine withdrawal results in upregulation of the pro-apoptotic Bim and induction of Caspase-3 associated apoptotic cell death, promoting deletion of activated commensal bacteria-specific T cells in a process we term “intestinal selection”, which parallels thymic selection. In contrast, commensal bacteria-specific CD4$^+$ T regulatory cells (T_{reg}) are not subject to ILC3-mediated deletion, potentially due to their ability to compete for IL-2, and migrate to the intestine whereby they further maintain tissue homeostasis in the presence of the commensal microflora.